Control of lateral migration and germ cell elimination by the *Drosophila melanogaster* lipid phosphate phosphatases Wunen and Wunen 2

Hiroko Sano, Andrew D. Renault, and Ruth Lehmann

Department of Cell Biology, Developmental Genetics Program, Skirball Institute of Biomolecular Medicine and Howard Hughes Medical Institute, New York University Medical Center, New York, NY 10016

In most organisms, primordial germ cells (PGCs) arise far from the region where somatic gonadal precursors (SGPs) are specified. Although PGCs in general originate as a single cluster of cells, the somatic parts of the gonad form on each site of the embryo. Thus, to reach the gonad, PGCs not only migrate from their site of origin but also split into two groups. Taking advantage of high-resolution real-time imaging, we show that in *Drosophila melanogaster* PGCs are polarized and migrate directionally toward the SGPs, avoiding the midline. Unexpectedly, neither PGC attractants synthesized in the SGPs nor known midline repellents for axon guidance were required to sort PGCs bilaterally. Repellent activity provided by *wunen* (*wun*) and *wunen-2* (*wun-2*) expressed in the central nervous system, however, is essential in this migration process and controls PGC survival. Our results suggest that expression of *wun/wun-2* repellents along the migratory paths provides faithful control over the sorting of PGCs into two gonads and eliminates PGCs left in the middle of the embryo.

Introduction

In many animals, primordial germ cells (PGCs) arise far from the region where their somatic partners are specified. In general, PGCs start as a group at one location and migrate toward a pair of somatic gonads. *Drosophila melanogaster* PGC migration provides an excellent system to analyze the behavior of migrating PGCs because both attractants and repellents that are expressed in the somatic tissues through which PGCs migrate have been identified.

In *D. melanogaster*, PGCs are formed at the posterior pole of the embryo attached to the posterior midgut (PMG) primordium (Williamson and Lehmann, 1996). During germband extension, PGCs are carried inside the embryo, which is where they begin active migration. PGCs initially migrate across the PMG. Subsequently, PGCs move from the PMG into the mesoderm, where they separate into bilateral clusters. This reorientation of PGCs is important for gonad formation as their final targets, the somatic gonadal precursors (SGPs), are specified on each side of the embryo in dorsolateral regions of the mesoderm of abdominal segments A4–A7. By the end of embryogenesis, PGCs and the SGPs are in close contact with each other and coalesce into embryonic gonads.

Genes that control PGC migration have been identified and ordered into steps according to their time of action. *trapped in endoderm-1*, which is a G protein–coupled receptor expressed in PGCs, is necessary for PGCs to cross the PMG (Kunwar et al., 2003; Santos and Lehmann, 2004a). After this transepithelial migration, two redundant genes, *wunen* (*wun*) and *wunen-2* (*wun-2*), guide the PGCs to the dorsal surface of the PMG (Zhang et al., 1997; Starz-Gaiano et al., 2001). *wun* and *wun-2* are expressed similarly in a variety of tissues, including the PMG, the central nervous system (CNS), and the epidermis (Zhang et al., 1997; Starz-Gaiano et al., 2001; Renault et al., 2002). In the PMG, both *wun* and *wun-2* are expressed ventrally, and PGCs migrate away from the site of *wun/wun-2* expression. *wun* and *wun-2* encode homologues of mammalian lipid phosphate phosphatases (LPPs), which are membrane-localized ectoenzymes whose catalytic domains face the outside of the cell to dephosphorylate extracellular phospholipid substrates (Zhang et al., 1997; Starz-Gaiano et al., 2001; Burnett and Howard, 2003). Our current hypothesis is that *wun* and *wun-2* create a gradient of a phospholipid through their restricted expression pattern and that PGCs migrate toward the region with the highest phospholipid levels (Starz-Gaiano et al., 2001; Renault et al., 2004; Santos and Lehmann, 2004a).

Correspondence to Ruth Lehmann: lehmann@saturn.med.nyu.edu

Abbreviations used in this paper: CNS, central nervous system; HMGCoAr, 3-hydroxy-3-methylglutaryl coenzyme A reductase; LPP, lipid phosphate phosphatase; PGC, primordial germ cell; PMG, posterior midgut; SGP, somatic gonadal precursor; *wun*, *wunen*; *wun-2*, *wunen-2*.

The online version of this article contains supplemental material.

The Journal of Cell Biology, Vol. 171, No. 4, November 21, 2005 675–683
http://www.jcb.org/cgi/doi/10.1083/jcb.200506038

Following their dorsal positioning on the PMG, PGCs move laterally and migrate away from the midline in the direction of the SGPs. The *hmgcr* gene, which encodes the enzyme 3-hydroxy-3-methylglutaryl coenzyme A reductase (HMGCoAr), has an important role in allowing PGCs to associate with the SGPs. *hmgcr* is expressed in a dynamic and tissue-specific pattern (Van Doren et al., 1998). In early stages of migration, *hmgcr* is broadly expressed in the lateral mesoderm, and then expression becomes restricted to the SGPs, which are specified in three clusters on both sides of the embryo. In *hmgcr* mutants, PGCs do not associate with the SGPs and misexpression of *hmgcr* can attract PGCs to ectopic tissues (Van Doren et al., 1998). A recent study showed that the isoprenoid branch in the *hmgcr* cascade, and the enzyme geranylgeranyl transferase type 1 in particular, is required for PGC migration, suggesting that geranylgeranylated proteins attract PGCs directly or that geranylgeranylation is indirectly required for synthesis or secretion of attractants (Santos and Lehmann, 2004a,b). Once the PGCs have contacted the SGPs, subsequent steps of gonad formation seem to be dictated by the somatic cells of the gonad (Brookman et al., 1992; Van Doren et al., 1998).

Although genetic analysis indicates that three pathways affect PGC migration, little is known about how PGCs migrate in vivo. Therefore, we used high-resolution real-time imaging to observe the PGC migratory path in a living embryo. We found that PGCs do not cross the midline once they exit the gut to move into bilateral groups. To explore the regulation of this migratory route in more detail, we analyzed known PGC attractant and repellent pathways, as well as midline guidance cues that are used during axon pathfinding. We found that repulsion by CNS-expressed *wun* and *wun-2* is required to move PGCs laterally and avoid the midline. Neither mutations in genes required for axonal pathfinding across the midline nor *hmgcr* and other putative attractants in the SGPs are required for lateral movement. We also found that PGCs left along the midline die in wild-type embryos via *wun/wun-2*–dependent cell death. These results show that *wun/wun-2* expressed in the CNS guides PGCs bilaterally and that continued exposure to Wun and Wun-2 leads to the elimination of mismigrating PGCs. Based on these results, we propose that Wun/Wun-2 are major regulators of PGC migration and that the dual functions of Wun/Wun-2 in repulsion and death confer faithful separation of PGCs into bilateral groups.

Results

PGCs do not cross the midline during the formation of bilateral gonads

Live imaging is a powerful tool in investigating the dynamics of migrating cells, as it allows the analysis of changes in cell shape, directionality, and speed over time. We combine live imaging with genetic analysis to detect new aspects of migrating PGCs and link them to the signaling systems that control PGC migration. To visualize PGCs in living embryos, an EGFP-moesin actin-binding domain fusion protein was expressed under the control of the *nanos* (*nos*) promoter, *nos* 5′UTR and 3′UTR regulatory regions (Dutta et al., 2002).

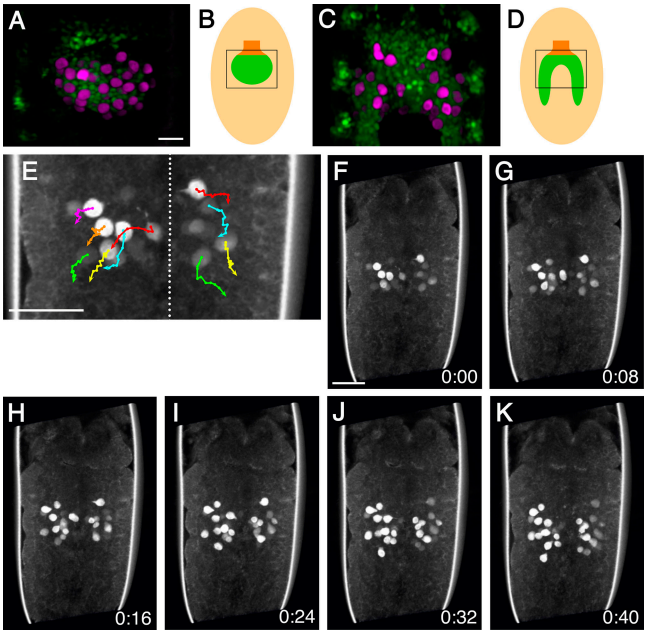

Figure 1. **PGCs do not cross the midline during the migration toward the lateral sides of the embryo.** (A–D) PGC migration from the PMG to the lateral sides of the embryo. PGCs were labeled with anti-Vasa antibody (purple), and the PMG was detected by the 1A121 enhancer-trap marker, which marks the midgut (green). (A) PGCs emerged throughout the posterior end of the PMG. (C) PGCs migrated laterally to form bilateral clusters. The regions of the embryo shown in A and B are indicated by the squares in B and D, respectively. (E–K) Time-lapse analysis of a living stage 10–11 embryo that expressed the EGFP-moesin fusion protein in PGCs. Trajectory of PGCs (E) and selected pictures (F–K) are presented. PGCs that were in the pocket or in the lumen of the PMG had a weaker signal, and the signal became stronger once they emerged. On the way to the lateral sides, they migrated directionally and did not cross the midline (dotted line in E). After 40 min, PGCs formed bilateral clusters. Embryos are oriented anterior to the top and dorsal to the front. Bars: (A) 20 μm; (E and F) 40 μm.

The moesin actin-binding domain localized the fusion protein to the cell membrane, which allowed us to trace the outline of the cell. In this system, we found that migrating PGCs displayed the morphological features of polarized, migrating cells, with fine cytoplasmic protrusions predominantly located at the leading edge of the cell and a broad uropod at the lagging edge of the cell (Fig. 1, E–K; see Fig. 3 A; and Videos 1 and 3, available at http://www.jcb.org/cgi/content/full/jcb.200506038/DC1). The appearance and general mode of migrating *D. melanogaster* PGCs resembles that of other individually migrating cells such as amebas, leukocytes, or neutrophils (Singer and Kupfer, 1986). Given the multitude of tissues that *D. melanogaster* PGCs migrate over and through, and the identified signaling pathways that guide their migration, *D. melanogaster* provides an excellent system to analyze the mechanisms of this type of cell migration in vivo.

In this study, we focus on the migratory step in which PGCs move away from the PMG toward the adjacent mesoderm. During this step PGCs split bisymmetrically. This is a crucial step in gonad formation as the SGPs are specified on each side of the embryo from the lateral mesoderm cells (Boyle and DiNardo, 1995). Static, fixed sections do not allow us to analyze this process in detail because this migration occurs

rapidly and the dynamics of cytoplasmic extensions cannot be followed. To determine the trajectories of migrating PGCs, we filmed embryos with time-lapse imaging and tracked the migratory path of each PGC (Fig. 1, E–K; and Video 1). We found that PGCs moved individually during their migration across the PMG and were evenly distributed along the posterior end of the PMG (Fig. 1, A, B, and E–K [dark cells]). Subsequently, PGCs reoriented toward the dorsal side of the embryo and displayed polarized morphology as they initiated lateral migration. Their large uropod, which marks the back of the cell, faced toward the midline, and they migrated straight to the lateral sides with few pauses (Fig. 1, E–K [bright cells]; and Video 1). 40 min after the onset of lateral migration, PGCs had segregated into separate cell clusters on either side of the embryo (Fig. 1, C, D, and E–K). Interestingly, PGCs seemed to avoid the midline, and none of them crossed it (Fig. 1 E and Video 1). To investigate the genetic control of this lateral movement, we tested several hypotheses. First, we tested whether lateral movement was controlled by known attractants, such as *hmgcr* in the lateral mesoderm and the SGPs; second, we tested whether lateral movement was regulated by guidance factors involved in axonal pathfinding along the midline; and third, we tested whether lateral movement was controlled by known PGC repellents.

PGC attractants in the mesoderm are not required to form bilateral clusters

HMGCoAr is the only factor identified so far that is necessary and sufficient for *D. melanogaster* PGC attraction (Van Doren et al., 1998). The *hmgcr* gene is expressed broadly in the lateral mesoderm during the period when PGCs migrate laterally and is restricted to the SGPs in later stages. To test a possible role of HMGCoAr in lateral sorting, we examined the phenotype of *hmgcr* mutant embryos and observed normal separation of PGCs into lateral clusters on each side of the embryo (Table I). To exclude a role of other attractant factors in the SGPs, we also tested the effect of ablating SGPs by using *abdominal-A* (*abd-A*) mutants in which SGPs are not specified (Brookman et al., 1992; Boyle and DiNardo, 1995). We found that PGCs sorted normally into bilateral groups in the absence of the SGPs (Table I). These results indicate that *hmgcr* and putative attractants in the SGPs are dispensable in the formation of bilateral clusters.

Midline genes required for axon guidance are not required for PGC lateral migration

We next asked whether midline repellents known to guide axons away from the midline act on PGCs during lateral migration. The best studied examples of midline repellents are *slit* (*sli*), *Netrin-A* (*NetA*), and *Netrin-B* (*NetB*) (Rothberg et al., 1988, 1990; Harris et al., 1996; Mitchell et al., 1996; Kidd et al., 1999). Neurons expressing either the Sli receptors *roundabout* (*robo*), *robo-2*, and *robo-3*, or the NetA and NetB receptor *unc-5*, do not cross the ventral midline and instead grow longitudinally along the midline (Kidd et al., 1998; Rajagopalan et al., 2000; Keleman and Dickson, 2001). The role of midline signaling has been extensively studied in axon guidance, however, it has not been investigated in gonad development.

Table I. **Formation of bilateral clusters in the mutant embryos**

Genotype	Number of PGCs in the middle of the embryo[a]	*n*	Significance[b]
Oregon R	2.3 ± 0.2	105	
hmgcr$^{26.31}$	3.1 ± 0.4	41	P > 0.2
hmgcr$^{26.31}$/*TM3*	3.5 ± 0.3	40	
abdA$^{46.51}$	5.8 ± 0.5	45	P > 0.2
abdA$^{46.51}$/*TM3*	5.3 ± 0.5	57	
sli^{2}	3.0 ± 0.4	44	P > 0.2
sli^{2}/*CyO*	2.7 ± 0.3	70	
NetA,B	3.3 ± 0.4	44	P > 0.2
NetA,B/FM7	3.7 ± 0.4	49	
sim^{2}	3.3 ± 0.4	73	P > 0.2
sim^{2}/*TM3*	3.5 ± 0.4	53	

[a]Embryos at early stage 11 were stained with anti-Vasa antibody. PGCs left in the middle of the embryo were counted.
[b]Probabilities were calculated by Fisher's exact probability test. Probabilities were compared (from top to bottom): *hmgcr*$^{26.31}$ with *hmgcr*$^{26.31}$/*TM3*, *abdA*$^{46.51}$ with *abdA*$^{46.51}$/*TM3*, *sli*^{2} with *sli*^{2}/*CyO*, *NetA,B* with *NetA,B/FM7*, and *sim*^{2} with *sim*^{2}/*TM3*.

We tested the effect of the loss of the *sli*, *NetA*, *NetB*, *robo*, and *robo-2* genes. We counted the number of lost PGCs in the middle of mutant embryos for each of these genes. The number of lost PGCs varied between lines, possibly because of the genetic background. However, we did not detect significant differences in the number of lost PGCs between homozygotes and heterozygotes of these mutants (Table I; unpublished data). To further explore the response of PGCs toward axonal guidance cues, we misexpressed *sli*, *NetA*, and *NetB* in the mesoderm, which is a tissue that normally attracts PGCs. PGCs were not repelled from the mesoderm and migrated normally (unpublished data), suggesting that these axonal repellents are not sufficient to repel PGCs when misexpressed. To determine whether additional, previously unknown repellents expressed in midline cells may promote lateral migration of PGCs, we eliminated the CNS midline lineage by using the *single-minded* (*sim*) mutation (Nambu et al., 1991). *sim* mutant embryos showed no obvious defect in lateral PGC migration (Table I). These results suggest that midline factors are not necessary to sort PGCs into bilateral clusters.

Lateral migration is regulated by Wun/Wun-2 LPPs

Previously, *wun* and *wun-2* were shown to act as repellents for migrating PGCs during their reorientation on the PMG just before their lateral migration. *wun* and *wun-2* expression is not restricted to the PMG, but is also observed in tissues such as the developing CNS and the epidermis (Zhang et al., 1997; Starz-Gaiano et al., 2001; Renault et al., 2002). We reasoned that *wun/wun-2* expression in the CNS could be a source of the repellent signal that directs PGCs laterally, as the CNS is located in two parallel rows flanking the midline of the embryo. In support of this hypothesis, we found that PGCs do not form lateral clusters in mutants that lack both *wun* and *wun-2;* instead, PGCs are scattered across the midline and throughout the embryo (see Fig. 4 C). To better understand the migration defects in *wun/wun-2* mutants, we observed migrating PGCs in

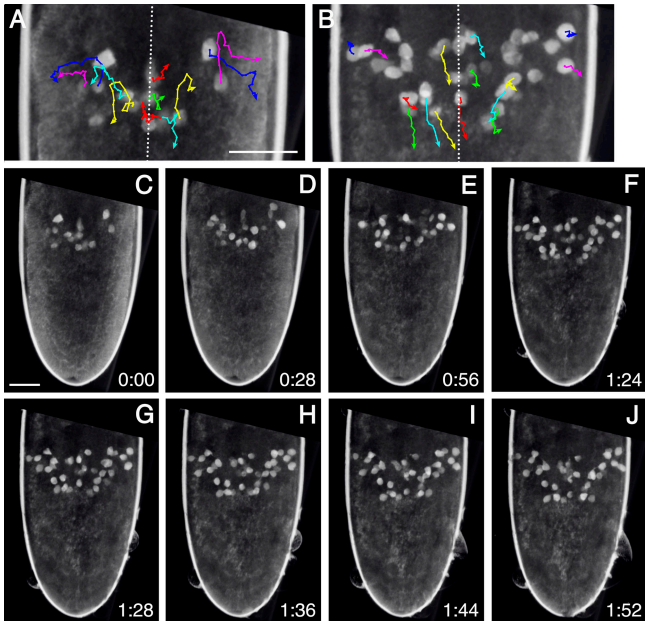

Figure 2. **PGCs cannot migrate laterally in the middle of the *wun/wun-2* embryo.** Time-lapse analysis of a *wun/wun-2* double mutant embryo. (A and C–F) At stage 10, PGCs emerged from the lumen of the PMG normally. However, PGCs did not migrate laterally and wandered in the middle of the embryo. PGCs in the lateral region migrated into the epidermis. A is a tracking for C–F. (B and G–J) At stage 11, PGCs stopped wandering and stayed at the same position while they continued to change cell shape. Anteroposterior movement is a consequence of germband retraction because the speed of malpighian tubules movement (0.5 μm/min) during germ band retraction is equal to the posterior movement of germ cells in *wun/wun-2* mutants. B is a tracking for G–J. Embryos are oriented anterior to the top and dorsal to the front. Bars, 40 μm.

living mutant embryos (Fig. 2 and Video 2, available at http://www.jcb.org/cgi/content/full/jcb.200506038/DC1). We found that PGCs behaved differently in *wun/wun-2* mutants depending on their location. PGCs in the middle portion of the PMG moved toward the mesoderm, but failed to change their position with respect to the midline (Fig. 2, A and C–F). PGCs in more lateral regions of *wun/wun-2* mutants continued to migrate laterally into the epidermis (Fig. 2, A and C–F). Although in wild-type embryos PGCs separated into bilateral groups within ∼40 min of leaving the PMG, PGCs in mutant embryos wandered for more than 1 h and failed to form bilateral clusters. Eventually, at a stage when wild-type PGCs had associated with the SGPs, mutant PGCs stopped wandering and remained in one location during germ band retraction (Fig. 2, B and G–J).

Although PGCs in the mutant did not migrate normally, they were clearly motile; they formed cytoplasmic extensions and migrated as fast as wild-type PGCs (Fig. 3, B and C; and Video 2). However, the morphology of PGCs in *wun/wun-2* mutants was different from that of wild-type PGCs. Wild-type PGCs consistently had a large, relatively stable protrusion at their lagging edge (Fig. 3, A [arrows], D, and E; and Video 3). In contrast, PGCs in the middle of *wun/wun-2* mutant embryos showed more cytoplasmic extensions (Fig. 3 D), including small protrusions (Fig. 3 B, arrowheads), as well as broad cytoplasmic extensions (Fig. 3 B, asterisks). In *wun/wun-2* mutant PGCs, cytoplasmic extensions are transient compared with extensions in wild-type PGCs (Fig. 3 E; and Video 4, available at http://www.jcb.org/cgi/content/full/jcb.200506038/DC1). PGCs in the lateral region of the mutants migrated further than those in the middle and eventually reached the epidermis, a tissue that also expresses *wun/wun-2* and that is normally devoid of PGCs. The morphology of lateral PGCs was more similar to that of wild-type PGCs (Fig. 3, C–E). These observations suggest that *wun/wun-2* mutants affect the lateral sorting of PGCs, but not their motility.

wun and *wun-2* expression in the CNS regulates lateral migration

wun and *wun-2* are expressed in various tissues including the gut, the CNS, and the epidermis (Zhang et al., 1997; Starz-Gaiano et al., 2001; Renault et al., 2002). To determine if the expression of *wun/wun-2* in the CNS is sufficient to explain the defect in lateral migration of *wun/wun-2* mutant embryos, we performed tissue-specific rescue experiments. For CNS-specific expression, we screened a collection of Gal4 insertion

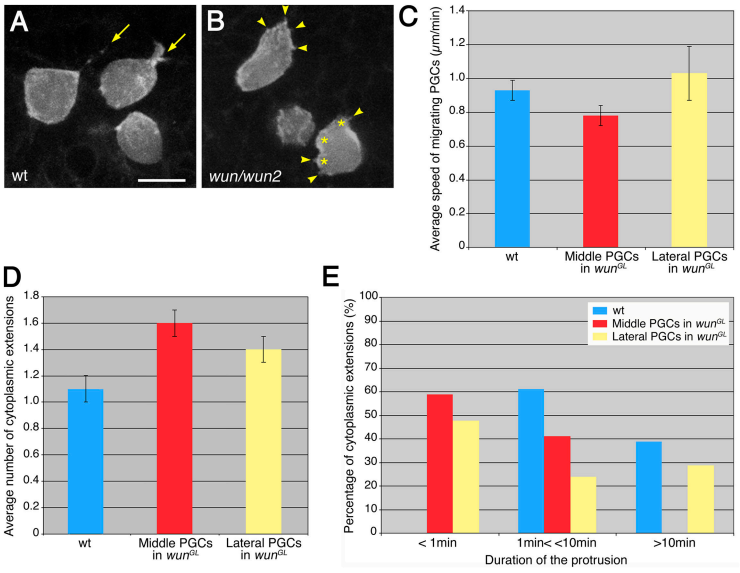

Figure 3. ***wun/wun-2* mutations affect the polarity of PGCs but not the motility.** (A and B) Morphology of migrating PGCs at stages 10 to 11. In wild type, PGCs were polarized with a large uropod at the lagging edge (arrows). (B) In *wun/wun-2* mutants, the morphology of PGCs in the middle region of the embryo was different from wild type. PGCs had several small cytoplasmic protrusions (arrowheads) as well as wide cytoplasmic extensions (asterisks). (C) The velocity of migrating PGCs was calculated. PGCs in the middle of *wun/wun-2* mutant embryos migrated slightly slower than PGCs in wild type. PGCs in the lateral regions of *wun/wun-2* mutant embryos migrated as fast as in wild type. (D) The average number of cytoplasmic extensions per PGC was counted. In *wun/wun-2* mutants, PGCs had more cytoplasmic extensions than in wild type. (E) Stability of cytoplasmic extensions in PGCs was examined during stages 10 and 11. In *wun/wun-2* mutants, duration of extensions in the middle PGCs was shorter than in wild-type PGCs. Cytoplasmic extensions of lateral PGCs in *wun/wun-2* mutants were more stable than middle PGCs but less stable than those in wild type. Bar, 10 μm. Error bars represent the standard error.

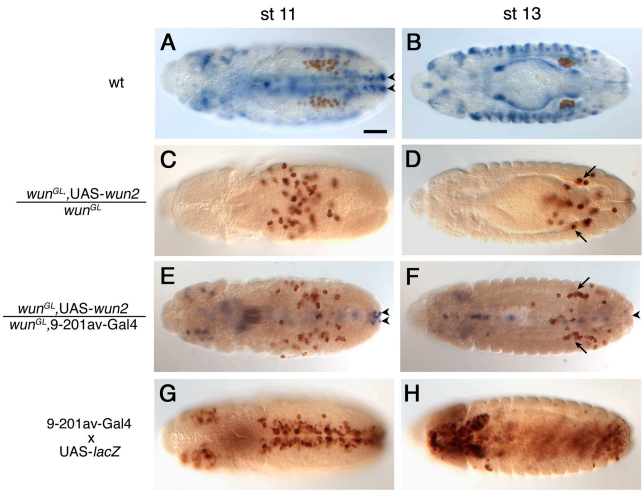

Figure 4. ***wun-2* expression in the CNS can rescue lateral migration in *wun/wun-2* embryos.** PGCs were labeled with anti-Vasa antibody (A–F; brown), and *wun-2* expression was detected by in situ hybridization (A, B, E, and F; blue). Embryos in the left panels are at stage 11, and those in the right panels are at stage 13. (A and B) In wild type, *wun-2* is expressed in the stripes of the CNS at stage 11 (arrowheads), and PGCs formed clusters at both lateral sides of the *wun-2* expression in the CNS (A). (B) At stage 13, PGCs coalesced to form the embryonic gonads. (C and D) Without *wun/wun-2* expression, PGCs were scattered at stage 11 and remained in the middle region (C). Only a small number of PGCs migrated to the gonads (D, arrows). (E and F) *wun-2* was expressed in the CNS using the 9-201av-Gal4 driver in a *wun/wun-2* background (arrowheads), resulting in more PGCs migrating into the gonads (arrows) than in *wun/wun-2* mutants (compare D and F). (G and H) 9-201av-Gal4 activity is expressed specifically in the CNS as detected by UAS-*lacZ* (brown). Bar, 50 μm.

lines (unpublished data) and identified one line, 9-201av-Gal4, which induces specific expression in the CNS (Fig. 4, G and H). CNS expression of *wun-2* driven by 9-201av-Gal4 restored bilateral sorting of PGCs in a *wun/wun-2* mutant background (Fig. 4, E and F, and Table II). However, rescue was not complete and not all PGCs reached a gonad (Fig. 4 F). One possibility is that *wun-2* expression driven by 9-201av-Gal4 did not faithfully reflect wild-type levels and timing of expression. Furthermore, the remaining migration defects could be because of the lack of *wun/wun-2* expression in other tissues such as the PMG and the epidermis, which may have prevented some PGCs from sensing Wun-2 expression in the CNS. We did not detect any patterning defects in the *wun/wun-2* mutant, suggesting that the remaining migration defects are not because of patterning defects (unpublished data). Together, our results demonstrate that *wun/wun-2* expression in the CNS acts as a repellent signal for the lateral migration of PGCs.

wun/wun-2–dependent cell death eliminates PGCs lost in the middle of the embryo

While monitoring PGC migration in wild type, we noted that PGCs that fail to sort laterally and remain in the middle of the embryo are smaller or fragmented, which is characteristic of dying cells (Fig. 5 A). We counted the number of dying PGCs at stage 12, which is when most PGCs have formed bilateral clusters. On average, seven PGCs remained in the middle of the embryo and ~30% of these PGCs were dying at this time point. Additional PGCs died during later stages, leading to a reduction of approximately eight PGCs during stages 11–13 (Table II). In contrast, of the 21 lateral PGCs only 0.2% were dying (Fig. 5 B). We did not detect dying PGCs in other tissues, suggesting that PGC death occurs mainly in the middle region of the embryo (Fig. 5 A and not depicted). Because PGCs die in proximity to the CNS where *wun* and *wun-2* are highly expressed, and the morphology of dying PGCs in the middle region is similar to that of dying PGCs in *wun*- or *wun-2*–overexpressed embryos (Fig. 5 A and not depicted), we reasoned that PGC death in the middle region might depend on *wun* and *wun-2* function. To test whether Wun and Wun-2 are required for elimination of mismigrating PGCs, we observed the death phenotype in *wun/wun-2* double mutants. In this experiment, we used wun^{GL}/Df(2R)NYX-D15, which is the strongest allelic combination of *wun* and *wun*-2 (Starz-Gaiano et al., 2001). We did not detect a significant reduction of PGCs during stage 10 (mean 37.0; standard error 0.9; $n = 26$) to stage 13 (34.1 ± 1.1; $n = 26$; one-way analysis of variance, $P > 0.05$), whereas sibling control embryos had a significant reduction of PGCs during stage 10 (33.0 ± 0.8; $n = 26$) to stage 13 (26.1 ± 0.8; $n = 26$; one-way analysis of variance, $P < 0.01$).

It was previously shown that PGC death induced by either overexpression of *wun/wun-2* in the soma or by lack of *wun-2* in PGCs is likely independent of apoptosis (Hanyu-Nakamura et al., 2004; Renault et al., 2004). In agreement with these results, we found that PGC death in the middle region occurred independent of the proapoptotic genes *head involution defective* (*hid*), *grim*, and *reaper* (Fig. 5 D) and was unaffected by inhibitors of apoptotic cell death, such as expression of the antiapoptotic gene *p35* in PGCs (Fig. 5 E).

We further characterized germ cell death induced by *wun-2* overexpression using the TUNEL assay. This method detects DNA strand breaks that are characteristically formed during apoptosis when nuclear DNA becomes fragmented by endogenous endonucleases. Although we can detect germ cells

Table II. ***wun-2* expression in the CNS can rescue lateral migration of PGCs in *wun/wun-2* mutants**

Genotype	Stage 11			Stage 13		
	PGCs in the middle of the embryo[a] (%)	Total number of PGCs	*n*	PGCs in the gonad (%)	Total number of PGCs	*n*
wun^{GL}, *UAS-wun-2*/wun^{GL}	20.5 ± 0.6 (52.2)	43.1 ± 0.9	26	6.4 ± 0.8 (17.0)	37.6 ± 1.6	21
wun^{GL}, *UAS-wun-2*/wun^{GL}, 9-201av-Gal4	17.5 ± 0.6 (39.0)	44.9 ± 1.3	27	19.1 ± 1.1 (48.1)	39.7 ± 1.1	23
wun^{GL}, *UAS-wun-2*/*CyO* or wun^{GL}/*CyO*	3.5 ± 0.5 (9.3)	37.6 ± 0.7	33	26.4 ± 0.8 (89.8)	29.4 ± 0.8	30

Embryos were stained with anti-Vas antibody.
[a]PGCs in the central one-third diameter of the embryo were counted.

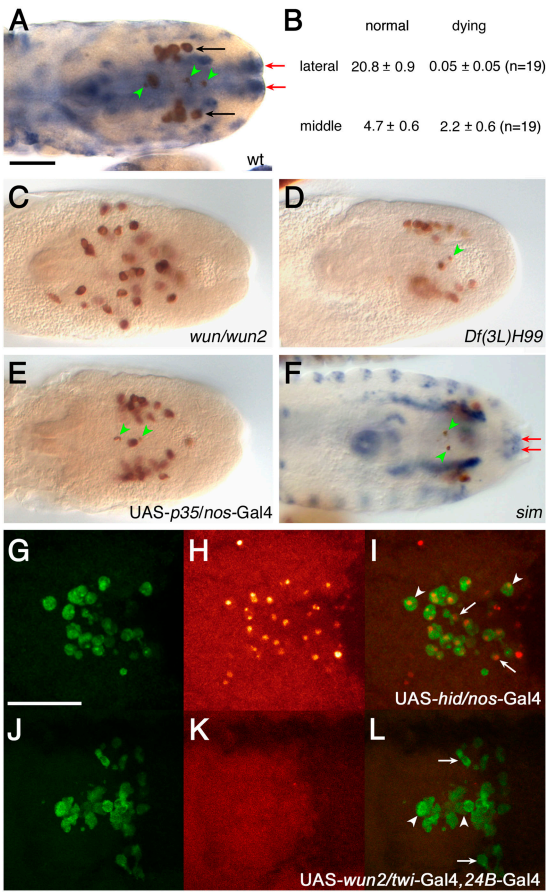

Figure 5. **PGCs that fail to migrate are eliminated by *wun/wun-2*–dependent cell death.** PGCs were labeled with anti-Vasa antibody (A and C–F, brown; and G–L, green), and *wun-2* mRNA was detected by in situ hybridization (A and F; blue). (A) Dying PGCs with small, fragmented shapes (green arrowheads) were in the region with high *wun-2* expression (red arrows). Few dying PGCs were detected in the lateral region where PGCs form clusters (black arrows). (B) The number (mean ± standard error) of normal and dying PGCs was counted in the lateral sides and in the middle of wild-type embryos at stage 12. (C) No dying PGCs were detected in *wun/wun-2* mutant embryos. (D and E) PGC death in the middle region was detected in *Df(3L)H99* and UAS-*p35/nos*-Gal4 embryos that lack apoptosis activity in PGCs. (F) *sim* mutant embryo. *wun-2* expression in the CNS was not affected (red arrows; out of focus in the posterior region), and PGC death occurred normally (green arrowheads). (G–L) Dorsal view with anterior to the left of stage 10 embryos showing TUNEL staining (H and K) of germ cells (G and J) dying because of either apoptosis through expression of *hid* in germ cells (G–I) or *wun-2* overexpression in the soma (J–L). (I and L) Merged images. Germ cells appearing regularly sized (arrowheads) and smaller and irregularly shaped (arrows) are positive for TUNEL when apoptosis is induced with UAS-*hid* (I) but not when death is induced by UAS-*wun-2* (L). Bars, 50 μm.

positive for TUNEL when we induce apoptosis through expression of *hid* in germ cells (65% positive out of 169 germ cells in 9 embryos between stages 9–11; Fig. 5 I), we were unable to detect TUNEL-positive germ cells when they were being killed through somatic overexpression of *wun-2* (0% of 200 germ cells in 15 embryos between stages 9–13; Fig. 5 L).

We also asked if midline genes had any effect on PGC survival. To remove the midline lineage, we used *sim* mutants and found that PGCs that remained in the middle were eliminated normally (Fig. 5 F). Furthermore, misexpressed *sli*, *NetA*, and *NetB* in the mesoderm did not kill PGCs (unpublished data). Together, these results show that midline genes are not required for PGC death, and that instead *wun* and *wun-2* are required to eliminate ectopic PGCs in the middle of the embryo in an apoptosis-independent manner.

Discussion

Using high-resolution in vivo imaging, we followed *D. melanogaster* PGCs as they emerged from the midgut and moved toward the SGPs. We found that PGCs are polarized during migration and that they move steadily toward the lateral mesoderm and SGPs. During this migration, PGCs sort into two bilateral groups, each group moving toward one set of SGP clusters. Genetic analysis of this process allowed us to make the following conclusions. First, Wun and Wun-2 LPP activity in the CNS acts as a long-range guidance factor during bilateral sorting and lateral migration of PGCs. Second, known axonal repellent guidance signals produced by ventral midline cells and PGC attractants produced by HMGCoAr-expressing cells in the lateral mesoderm and SGPs are not required for lateral migration. Finally, high levels of Wun and Wun-2 in the CNS eliminate PGCs that fail to sort properly from the middle. We conclude that *D. melanogaster* LPPs play a major role in guiding *D. melanogaster* germ cells to the bilateral gonads and eliminating germ cells left at the midline. Our data suggest repulsion and midline exclusion as an alternate mechanism to attraction and protection during the lateral sorting of germ cells.

Wun/Wun-2 repellents in the CNS are essential for bilateral sorting of PGCs

Our time-lapse analysis showed that PGCs start migrating laterally soon after they emerge from the PMG and, thus, before SGPs are specified. Consistent with this finding, PGCs sort bilaterally in *abd-A* mutants that lack SGPs. Because PGCs fail to leave the gut in mutants lacking lateral mesoderm, we were unable to test if lateral mesoderm, by itself, is required for the lateral migration of PGCs (Broihier et al., 1998). Instead, we tested the ability of PGCs to divide into two groups in *hmgcr* mutants because *hmgcr* is broadly expressed in the lateral mesoderm and plays an important role in PGC attraction (Van Doren et al., 1998). *hmgcr* mutants did not show defects in lateral migration, suggesting that attraction by *hmgcr* is not critical for bilateral sorting. Finally, it is conceivable that as the PGCs are leaving the PMG, the movement of the developing PMG toward the mesoderm squeezes PGCs into two groups, thereby indirectly causing bilateral cluster formation. However, this is unlikely because in embryos doubly mutant for the integrin βPS and integrin β*v* the morphological changes of the PMG do not occur but the two gonads form normally (Devenport and Brown, 2004). Together, the fact that neither *abd-A* or *hmgcr* mutants nor embryos that fail to undergo normal midgut morphogenesis affect the bilateral movement of PGCs suggests that neither physical guidance nor attraction play a major role in lateral sorting of PGCs.

Instead, *wun/wun-2* expression in the CNS is required to generate lateral clusters of PGCs by repulsion. High-resolution live imaging demonstrated that *wun/wun-2* mutations affect the

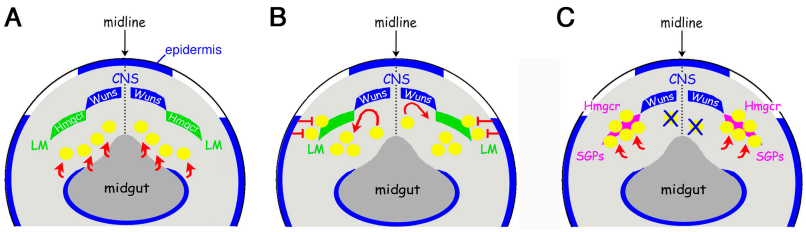

Figure 6. **Model for the guidance of PGCs to the SGPs.** (A) At stage 10, Wun and Wun-2 (blue) expressed in the ventral side of the PMG move PGCs (yellow) to the dorsal surface of the PMG. Hmgcr and other unknown factors expressed in the lateral mesoderm (LM; green) attract PGCs from the PMG. (B) CNS-expressed Wun and Wun-2 repel PGCs and promote lateral migration. Wun and Wun-2 also prevent PGCs from migrating into the epidermis. (C) Consequently, PGCs are close to the SGPs (pink) and would be more easily captured by SGPs. PGCs that fail to migrate and remain in the middle of the embryo are eliminated by the high amounts of Wun and Wun-2 expressed in the CNS. The dorsal half of the embryo is shown.

polarity but not the motility of PGCs. This change in morphology was particularly striking among cells that remained in the middle of the embryo, whereas more lateral cells continued to migrate toward the epidermis. Loss of polarity was accompanied by more frequent and less stable cytoplasmic extensions within a given time frame, slightly slower velocity, and overall shorter tracking distance. PGCs that exited the gut from a more lateral position in *wun/wun-2* embryos had a more normal morphology and migrated into the epidermis. One possible interpretation of these results is that PGCs in more medial locations are in a generally attractive environment produced by *hmgcr* expression and possibly other attractants and that this environment may cause germ cells to stop migrating. PGCs in more lateral regions, on the other hand, may not experience sufficient levels of attractants and therefore continue to migrate. It remains open whether this migration is directed by specific somatic cues and if so what these cues are. Because these lateral PGCs in *wun/wun-2* mutants often end up in the epidermis, it is likely that *wun/wun-2* expression in the epidermis of wild-type embryos repels PGCs. *wun* and *wun-2* expression in the gut, CNS, and epidermis flank the migratory route of PGCs. This and the striking defects in migration observed in *wun/wun-2* mutants suggest that Wun/Wun-2 is a major long-range guidance factor that guides PGCs toward the two gonads. Based on our observations, we propose that dynamic expression of *wun/wun-2* guides PGCs successively: first to reorient them dorsally on the midgut, then to move them from the gut into the mesoderm, and finally to steer them toward the lateral mesoderm and the SGPs away from the ventral midline, the CNS, and the epidermis (Fig. 6).

Wun and Wun-2 activity eliminates PGCs trapped in the middle of the embryo

We found that *wun/wun-2* expression in the CNS not only repels PGCs away from the midline but is also responsible for the elimination of ectopic PGCs that failed to sort bilaterally. These results demonstrate a role for somatic *wun/wun-2* in normal PGC survival that had previously been revealed only after overexpression of either *wun* or *wun-2* in the soma (Starz-Gaiano et al., 2001). In our rescue experiment, *wun-2* expression driven by 9-201av-Gal4 rescued lateral migration but not death in the middle of the embryo (Fig. 4 and Table II). These results suggest that low levels of Wun/Wun-2 are sufficient to direct migration away from Wun/Wun-2–expressing cells, whereas continuous and possible high levels of exposure to Wun/Wun-2 leads to elimination of PGCs. Wun and Wun-2 are likely to regulate the distribution of a phospholipid substrate. PGCs may migrate along a gradient toward high levels of phospholipids, whereas low, evenly sustained levels of phospholipid may be sufficient for survival.

It is unclear why PGCs need to be removed from the middle region of *D. melanogaster* embryos because teratomas, similar to those observed in mouse and humans, do not seem to originate from lost PGCs in flies (Underwood et al., 1980). However, it was recently reported that PGCs are able to transdifferentiate into somatic cells when they lack the translational regulator Nanos (Hayashi et al., 2004). In this case, PGCs have to be prevented from apoptotic death. Interestingly, apoptotic death of *D. melanogaster* PGCs has so far only been observed in mutant backgrounds, such as *nanos,* which causes inappropriate somatic gene expression in PGCs (Hayashi et al., 2004). Our data show that a nonapoptotic death pathway acts during PGC elimination in the middle of the embryo. There is no evidence that PGCs lose their germ cell character in *wun/wun-2* mutants, and thus this pathway may be specific to germ cells. In mouse, ectopic PGCs are eliminated by apoptotic death (Stallock et al., 2003). It will be interesting to see whether nonapoptotic pathways, mediated by LPPs similar to Wun/Wun-2, also play a role in the control of germ cell survival in vertebrates.

Bilateral sorting of PGCs

In most organisms germ cells originate at one location, whereas the somatic gonad forms bilaterally. Thus, sorting of germ cells along the midline is a conserved phenomenon. Furthermore, elimination of germ cells trapped at the midline is an important aspect of normal development, as germ cells trapped in the midline have been shown to give rise to germ line teratomas, one of the most frequent cancers among young adults (Oosterhuis and Looijenga, 2005). Like *D. melanogaster* PGCs, zebrafish and mouse PGCs migrate away from the dorsal midline (De Robertis and Sasai, 1996) toward the genital ridge (Weidinger et al., 1999; McLaren, 2003). Repellents involved in this process have yet to be reported in zebrafish and mouse. It was shown that migration to the genital ridge is controlled by the G protein–coupled receptor CXCR4 and its ligand SDF-1 in both animals (Doitsidou et al., 2002; Ara et al., 2003; Knaut et al., 2003; Molyneaux et al., 2003; Santos and Lehmann, 2004a). CXCR4 is expressed in migrating PGCs, and SDF-1 is expressed in the somatic tissues and acts as an attractant. SDF-1 changes its expression pattern during embryonic development

as it prefigures the route of PGC migration and, at least in zebrafish, seems to be the major guidance signal for PGCs. In CXCR4 mutant mice, germ cells that lack the receptor remain in the midline and die, presumably because of the lack of survival factors provided by the genital ridges (Molyneaux et al., 2003; Santos and Lehmann, 2004a). Thus, in mouse, attractants and survival factors seem to be the major determinants that sort PGCs into two clusters, whereas in *D. melanogaster* repellents and death dominate. Given the striking similarity in PGC behavior, it will be interesting to see if these disparities are because of differences in signaling mechanisms or reflect evolutionary changes in guidance strategy.

Materials and methods

Fly stocks

To label PGCs in a live embryo, the P_{nos}*::egfp-moe::nos* 3′UTR construct was introduced into the fly genome. In the transgenic flies, EGFP fused with the actin-binding domain of the moesin protein was expressed under the control of the maternal *nos* promoter. The RNA, and thus the fusion protein, are localized at the posterior pole of the embryo by the function of *nos* 3′ UTR (Gavis and Lehmann, 1992; Dutta et al., 2002).

The following mutants were used: wun^{CE} and $Df(2R)wun^{GL}$ (K. Howard, University College London, London, UK) are strong alleles that affect both *wun* and *wun-2* genes (Zhang et al., 1996). *Df(2R)NYX-D15* lacks *wun* and *wun-2* (Starz-Gaiano et al., 2001). Throughout the text we refer to *wun* and *wun-2* double mutant as *wun/wun-2*. $hmgcr^{26.31}$ and $abdA^{46.51}$ were identified in the screen by Moore et al. (1998). sli^{2} and sim^{2} (Bloomington Stock Center, Bloomington, IN; B. Dickson, Research Institute of Molecular Pathology, Vienna, Austria) are null alleles of the *sli* or *sim* genes, respectively (Thomas et al., 1988; Sonnenfeld and Jacobs, 1994; Kidd et al., 1999). *Df(1)NP5* (B. Dickson) was used as a null allele of the *NetA* and *NetB* genes (Mitchell et al., 1996). $robo^{1}$ (B. Dickson) is a null allele for *robo* gene (Kidd et al., 1998). $robo2^{1}$, $robo2^{4}$, and $robo2^{8}$ (B. Dickson) are null alleles for *robo2* (Rajagopalan et al., 2000). 1A121 (R. Reuter, Universität Tübingen, Tübingen, Germany) is an enhancer trap marker in which β-galactosidase is expressed, mainly in the midgut (Reuter, 1994). In the overexpression experiments, UAS-*wun-2*, UAS-*hmgcr*, UAS-*NetA*, UAS-*NetB* (B. Dickson), and UAS-*sli* (Bloomington Stock Center) were used (Mitchell et al., 1996; Van Doren et al., 1998; Kidd et al., 1999; Starz-Gaiano et al., 2001). To express the transgene in the CNS, we screened Gal4 insertion lines obtained from U. Heberlein (University of California, San Francisco, San Francisco, CA) and identified 9-201av-Gal, which is specific for the CNS. We used *twi*-Gal4*; 24B*-Gal4 (M. Akam, University of Cambridge, Cambridge, UK) for mesodermal expression and 69B-Gal4 (Bloomington Stock Center) for epidermal expression (Brand and Perrimon, 1993; Riechmann et al., 1997).

Real-time imaging

Embryos were mounted in Halocarbon Oil 200 on standard membrane (YSI Inc.) and covered with a coverslip. Images were acquired at RT on a microscope (model Eclipse E600FN; Nikon) with a Radiance system (Bio-Rad Laboratories) and a 10-W pumped laser (model Tsunami; Spectra-Physics). In Videos 1 and 2, embryos were scanned with a 40× objective (Nikon; Plan Fluor, NA 0.75) with a spacing of 1.95 μm between frames. In Videos 3 and 4, the scan was done with a 60× objective (Nikon; Plan Apo, Water, NA 1.2) with a 1.05-μm spacing between frames. To track the trajectory of PGCs, this procedure was repeated every 2 min (Videos 1 and 2). To analyze speed and stability of cytoplasmic extensions in wild-type PGCs, embryos were filmed every 1 min (Video 3). Because cytoplasmic extensions of *wun/wun-2* mutant PGCs move rapidly, *wun/wun-2* embryos were filmed every 30 s (Video 4). Images were acquired using LaserSharp 2000 software (Bio-Rad Laboratories) and were reconstructed into three-dimensional movies by Volocity 2.5.1 software (Improvision). PGCs were tracked manually using Photoshop software (Adobe).

Immunostaining and in situ hybridization

Embryos were fixed for 30 min in 4% formaldehyde, devitellinized using heptane/methanol, and stained using standard protocols. Rabbit anti-Vasa antibody (1:20,000) was used to detect PGCs. The 1A121 enhancer-trap marker was detected with monoclonal antibody against β-galactosidase (1:1,000; Promega). Secondary antibodies used were biotinylated goat anti–rabbit antibody (1:500; Jackson ImmunoResearch Laboratories), Alexa Fluor 488–conjugated goat anti–mouse and anti–rabbit antibodies (1:500; Invitrogen), Alexa Fluor 568–conjugated goat anti–mouse antibody (1:4,000; Invitrogen), and mouse Cy3-conjugated anti-digoxigenin antibody (1:500). In situ hybridization was performed as described in Kobayashi et al. (1999). Fluorescently labeled embryos were mounted in Aqua-Poly/Mount (Polysciences, Inc.) and imaged on a confocal microscope (model DM RBE; Leica) with a 40× objective (Leica; Plan Apo, NA 1.25–0.75), using the TCS NT program (Leica). Immunohistochemically labeled embryos were mounted in Polybed812 (Polysciences, Inc.) and analyzed with an Axiophot microscope using a 20× objective (both Carl Zeiss MicroImaging, Inc.; NeoFluor, NA 0.5). Photographs were taken with a color mosaic camera (model Insight 14.2; Diagnostic Instruments) using Spot2.4 Software (Diagnostic Instruments).

TUNEL assay

For TUNEL labeling, embryos were fixed as described in the immunostaining and in situ hybridization section and, after rehydration in phosphate buffered saline with 0.1% Tween 20 (PBST), proteinase K–treated (10 μg/ml) for 5 min, washed four times for 5 min in PBST, and fixed again in 4% formaldehyde for 20 min. After four 5-min washes of PBST, apoptotic cells were labeled with digoxigenin using the ApopTag kit (CHEMICON International, Inc.) as follows. Embryos were incubated in equilibration buffer for 1 h and in 2:1 reaction buffer/TdT enzyme with Triton X-100 added to 0.3% at 37°C overnight. The labeling reaction was stopped with a 5-min incubation with 34:1 water/stop buffer. The embryos were then stained for Vasa and digoxigenin as described in the immunostaining and in situ hybridization section.

To induce apoptosis in germ cells, we used embryos laid by *nosGAL4VP16* females mated to UAS-*hid* males. To examine germ cells dying by *wun-2* overexpression in the soma, we examined embryos laid by *twiGAL4;24BGal4* females mated to UAS-*wun-2* males. Pictures shown were acquired on a confocal microscope as described in Immunostaining and in situ hybridization and are maximum intensity projections of a stack made with a Z interval of 2 μm using ImageJ 1.34s software (National Institutes of Health).

Online supplemental material

Table S1 shows that in *wun/wun-2* mutant embryo germ cells seem to migrate at different speeds dependent on their position within the embryo, whereby lateral germ cells move faster than more centrally located germ cells (Fig. 3 C). Table S2 shows that the number of cytoplasmic protrusions in a given germ cell per time point is increased in *wun/wun-2* mutant embryos compared with wild type. This finding is consistent with an apparent loss of directed migration and polarized morphology in the mutants (Videos 2 and 4; and Fig. 3 D). Table S3 shows that cytoplasmic protrusions in a given germ cell per time point are less stable in *wun/wun-2* mutant embryos as compared with wild type. This finding is consistent with an apparent loss of directed migration and polarized morphology in the mutants (Videos 2 and 4; and Fig. 3 E).

Videos 1 and 2 show migration of germ cells in a wild-type (Video 1) and a *wun/wun-2* mutant embryo (Video 2) at the stage when germ cells leave the midgut and enter the mesoderm. Videos 3 and 4 are shown at higher magnification to observe migratory morphology of single germ cells in a wild-type (Video 3) and a *wun/wun-2* mutant embryo (Video 4) as they move from the midgut into the mesoderm. Online supplemental material is available at http://www.jcb.org/cgi/content/full/jcb.200506038/DC1.

We would like to thank our colleagues and the Bloomington Stock Center for the fly stocks and antibodies, as listed in the text. We also thank Dr. U. Heberlein for the Gal4 lines, and D. Siekhaus, P. Kunwar, A. Sudarov, S. Wang, and M. Haesemeyer for the Gal4 screen. We are grateful to Drs. M. Dustin and W. Gan for use of their two-photon microscope and to both them and their lab members, Julie Huang in particular, for their help with imaging. Thanks also to members of our laboratory for critical comments on the manuscript.

This work was supported by National Institutes of Health grant HD49100. A.D. Renault is a Charles H. Revson Senior Fellow in Biomedical Science and R. Lehmann is a Howard Hughes Medical Institute investigator.

Submitted: 6 June 2005
Accepted: 18 October 2005

References

Ara, T., Y. Nakamura, T. Egawa, T. Sugiyama, K. Abe, T. Kishimoto, Y. Matsui, and T. Nagasawa. 2003. Impaired colonization of the gonads by primordial germ cells lacking a chemokine, stromal cell-derived factor-1 (SDF-1). *Proc. Natl. Acad. Sci. USA.* 100:5319–5323.

Boyle, M., and S. DiNardo. 1995. Specification, migration and assembly of the somatic cells of the *Drosophila* gonad. *Development.* 121:1815–1825.

Brand, A.H., and N. Perrimon. 1993. Targeted gene expression as a means of altering cell fates and generating dominant phenotypes. *Development.* 118:401–415.

Broihier, H.T., L.A. Moore, M. Van Doren, S. Newman, and R. Lehmann. 1998. *zfh-1* is required for germ cell migration and gonadal mesoderm development in *Drosophila*. *Development.* 125:655–666.

Brookman, J.J., A.T. Toosy, L.S. Shashidhara, and R.A. White. 1992. The 412 retrotransposon and the development of gonadal mesoderm in *Drosophila*. *Development.* 116:1185–1192.

Burnett, C., and K. Howard. 2003. Fly and mammalian lipid phosphate phosphatase isoforms differ in activity both *in vitro* and *in vivo*. *EMBO Rep.* 4:793–799.

De Robertis, E.M., and Y. Sasai. 1996. A common plan for dorsoventral patterning in Bilateria. *Nature.* 380:37–40.

Devenport, D., and N.H. Brown. 2004. Morphogenesis in the absence of integrins: mutation of both *Drosophila* beta subunits prevents midgut migration. *Development.* 131:5405–5415.

Doitsidou, M., M. Reichman-Fried, J. Stebler, M. Koprunner, J. Dorries, D. Meyer, C.V. Esguerra, T. Leung, and E. Raz. 2002. Guidance of primordial germ cell migration by the chemokine SDF-1. *Cell.* 111:647–659.

Dutta, D., J.W. Bloor, M. Ruiz-Gomez, K. VijayRaghavan, and D.P. Kiehart. 2002. Real-time imaging of morphogenetic movements in *Drosophila* using Gal4-UAS-driven expression of GFP fused to the actin-binding domain of moesin. *Genesis.* 34:146–151.

Gavis, E.R., and R. Lehmann. 1992. Localization of *nanos* RNA controls embryonic polarity. *Cell.* 71:301–313.

Hanyu-Nakamura, K., S. Kobayashi, and A. Nakamura. 2004. Germ cell-autonomous Wunen2 is required for germline development in *Drosophila* embryos. *Development.* 131:4545–4553.

Harris, R., L.M. Sabatelli, and M.A. Seeger. 1996. Guidance cues at the *Drosophila* CNS midline: identification and characterization of two *Drosophila* Netrin/UNC-6 homologs. *Neuron.* 17:217–228.

Hayashi, Y., M. Hayashi, and S. Kobayashi. 2004. Nanos suppresses somatic cell fate in *Drosophila* germ line. *Proc. Natl. Acad. Sci. USA.* 101: 10338–10342.

Keleman, K., and B.J. Dickson. 2001. Short- and long-range repulsion by the *Drosophila* Unc5 Netrin receptor. *Neuron.* 32:605–617.

Kidd, T., K. Brose, K.J. Mitchell, R.D. Fetter, M. Tessier-Lavigne, C.S. Goodman, and G. Tear. 1998. Roundabout controls axon crossing of the CNS midline and defines a novel subfamily of evolutionarily conserved guidance receptors. *Cell.* 92:205–215.

Kidd, T., K.S. Bland, and C.S. Goodman. 1999. Slit is the midline repellent for the Robo receptor in *Drosophila*. *Cell.* 96:785–794.

Knaut, H., C. Werz, R. Geisler, and C. Nusslein-Volhard. 2003. A zebrafish homologue of the chemokine receptor *Cxcr4* is a germ-cell guidance receptor. *Nature.* 421:279–282.

Kobayashi, S., R. Amikura, A. Nakamura, and P. Lasko. 1999. Techniques for analyzing protein and RNA distribution in *Drosophila* ovaries and embryos at structural and ultrastructural resolution. *In* A Comparative Methods Approach to the Study of Oocyte and Embryos. J.D. Richter, editor. Oxford University Press, New York. 426–445.

Kunwar, P.S., M. Starz-Gaiano, R.J. Bainton, U. Heberlein, and R. Lehmann. 2003. Tre1, a G protein-coupled receptor, directs transepithelial migration of *Drosophila* germ cells. *PLoS Biol.* 1:372–384.

McLaren, A. 2003. Primordial germ cells in the mouse. *Dev. Biol.* 262:1–15.

Mitchell, K.J., J.L. Doyle, T. Serafini, T.E. Kennedy, M. Tessier-Lavigne, C.S. Goodman, and B.J. Dickson. 1996. Genetic analysis of *Netrin* genes in *Drosophila*: Netrins guide CNS commissural axons and peripheral motor axons. *Neuron.* 17:203–215.

Molyneaux, K.A., H. Zinszner, P.S. Kunwar, K. Schaible, J. Stebler, M.J. Sunshine, W. O'Brien, E. Raz, D. Littman, C. Wylie, and R. Lehmann. 2003. The chemokine SDF1/CXCL12 and its receptor CXCR4 regulate mouse germ cell migration and survival. *Development.* 130:4279–4286.

Moore, L.A., H.T. Broihier, M. Van Doren, and R. Lehmann. 1998. Gonadal mesoderm and fat body initially follow a common developmental path in *Drosophila*. *Development.* 125:837–844.

Nambu, J.R., J.O. Lewis, K.A. Jr. Wharton, and S.T. Crews. 1991. The *Drosophila* single-minded gene encodes a helix-loop-helix protein that acts as a master regulator of CNS midline development. *Cell.* 67:1157–1167.

Oosterhuis, J.W., and L.H. Looijenga. 2005. Testicular germ-cell tumours in a broader perspective. *Nat. Rev. Cancer.* 5:210–222.

Rajagopalan, S., V. Vivancos, E. Nicolas, and B.J. Dickson. 2000. Selecting a longitudinal pathway: Robo receptors specify the lateral position of axons in the *Drosophila* CNS. *Cell.* 103:1033–1045.

Renault, A.D., M. Starz-Gaiano, and R. Lehmann. 2002. Metabolism of sphingosine 1-phosphate and lysophosphatidic acid: a genome wide analysis of gene expression in *Drosophila*. *Mech. Dev.* 119:S293–S301.

Renault, A.D., Y.J. Sigal, A.J. Morris, and R. Lehmann. 2004. Soma-germ line competition for lipid phosphate uptake regulates germ cell migration and survival. *Science.* 305:1963–1966.

Reuter, R. 1994. The gene *serpent* has homeotic properties and specifies endoderm versus ectoderm within the *Drosophila* gut. *Development.* 120:1123–1135.

Riechmann, V., U. Irion, R. Wilson, R. Grosskortenhaus, and M. Leptin. 1997. Control of cell fates and segmentation in the *Drosophila* mesoderm. *Development.* 124:2915–2922.

Rothberg, J.M., D.A. Hartley, Z. Walther, and S. Artavanis-Tsakonas. 1988. *slit*: an EGF-homologous locus of *D. melanogaster* involved in the development of the embryonic central nervous system. *Cell.* 55:1047–1059.

Rothberg, J.M., J.R. Jacobs, C.S. Goodman, and S. Artavanis-Tsakonas. 1990. *slit*: an extracellular protein necessary for development of midline glia and commissural axon pathways contains both EGF and LRR domains. *Genes Dev.* 4:2169–2187.

Santos, A.C., and R. Lehmann. 2004a. Germ cell specification and migration in *Drosophila* and beyond. *Curr. Biol.* 14:R578–R589.

Santos, A.C., and R. Lehmann. 2004b. Isoprenoids control germ cell migration downstream of HMGCoA reductase. *Dev. Cell.* 6:283–293.

Singer, S.J., and A. Kupfer. 1986. The directed migration of eukaryotic cells. *Annu. Rev. Cell Biol.* 2:337–365.

Sonnenfeld, M.J., and J.R. Jacobs. 1994. Mesectodermal cell fate analysis in *Drosophila* midline mutants. *Mech. Dev.* 46:3–13.

Stallock, J., K. Molyneaux, K. Schaible, C.M. Knudson, and C. Wylie. 2003. The pro-apoptotic gene Bax is required for the death of ectopic primordial germ cells during their migration in the mouse embryo. *Development.* 130:6589–6597.

Starz-Gaiano, M., N.K. Cho, A. Forbes, and R. Lehmann. 2001. Spatially restricted activity of a *Drosophila* lipid phosphatase guides migrating germ cells. *Development.* 128:983–991.

Thomas, J., S.T. Crews, and C.S. Goodman. 1988. Molecular genetics of the single-minded locus: a gene involved in the development of the *Drosophila* nervous system. *Cell.* 52:133–141.

Underwood, E.M., J.H. Caulton, C.D. Allis, and A.P. Mahowald. 1980. Developmental fate of pole cells in *Drosophila melanogaster*. *Dev. Biol.* 77:303–314.

Van Doren, M., H.T. Broihier, L.A. Moore, and R. Lehmann. 1998. HMG-CoA reductase guides migrating primordial germ cells. *Nature.* 396:466–469.

Weidinger, G., U. Wolke, M. Koprunner, M. Klinger, and E. Raz. 1999. Identification of tissues and patterning events required for distinct steps in early migration of zebrafish primordial germ cells. *Development.* 126:5295–5307.

Williamson, A., and R. Lehmann. 1996. Germ cell development in *Drosophila*. *Annu. Rev. Cell Dev. Biol.* 12:365–391.

Zhang, N., J. Zhang, Y. Cheng, and K. Howard. 1996. Identification and genetic analysis of *wunen*, a gene guiding *Drosophila melanogaster* germ cell migration. *Genetics.* 143:1231–1241.

Zhang, N., J. Zhang, K.J. Purcell, Y. Cheng, and K. Howard. 1997. The *Drosophila* protein Wunen repels migrating germ cells. *Nature.* 385:64–67.